J. Fluid Mech. (2006), *vol.* 567, *pp.* 91–110. © 2006 Cambridge University Press
doi:10.1017/S0022112006002114 Printed in the United Kingdom

Local stability of the Abrashkin–Yakubovich family of vortices

By D. GUIMBARD AND S. LEBLANC

LSEET, Université du Sud Toulon-Var, BP 20132, 83957 La Garde cedex, France

(Received 3 May 2005 and in revised form 14 April 2006)

The three-dimensional stability of the family of two-dimensional inviscid vortex patches discovered by Abrashkin & Yakubovich (*Sov. Phys. Dokl.* vol. 29, 1984, p. 370) is explored. Generally unsteady and non-uniform, these bounded regions of vorticity evolve freely in a surrounding irrotational flow. This family of solutions includes the Rankine circular vortex, Kirchhoff's ellipse, and freely rotating polygonal vortices as special cases. Taking advantage of their Lagrangian description, the stability analysis is carried out with the theory of local instabilities. It is shown that, apart from the Rankine vortex, these flows are three-dimensionally unstable. Background rotation or density stratification may however be stabilizing.

1. Introduction

There have been considerable developments in stability theory thanks to the discovery of elliptical instability. This instability alters the evolution of vortices or coherent structures in shear flows once their streamlines are locally elliptical (Bayly, Orszag & Herbert 1988; Huerre & Rossi 1998; Cambon & Scott 1999; Kerswell 2002). In 1987, Bayly pointed out that elliptical instability and other mechanisms such as centrifugal or columnar vortex instabilities could be described by an unified approach; he wrote: "The common features of these broadband instabilities suggest that they are all special cases of a very general phenomenon, and that a theory broad enough to comprehend these effects would lead to new insights into instabilities of other flows as well" (Bayly 1987). The approach he formulated and developed in parallel with Eckhoff & Storesletten (1978), Friedlander & Vishik (1991), and Lifschitz & Hameiri (1991) is the theory of local (or short-wave) instabilities, which led to the discovery of some new instability mechanisms (Friedlander & Lipton-Lifschitz 2003).

The present paper deals with the stability of a class of two-dimensional exact solutions of the Euler equations discovered by Abrashkin & Yakubovich (1984). Described in a Lagrangian representation, the solution of Abrashkin & Yakubovich includes Gerstner's waves as a special case. It also describes a family of generally non-uniform and unsteady vortex patches that evolve freely in a surrounding irrotational flow at rest at infinity. Rankine's circular vortex and Kirchhoff's ellipse enter that category, as steadily rotating polygonal vortex patches with non-uniform vorticity distributions.

It is well-known that the self-induced rotation of Kirchhoff's ellipse may be stopped by imposing an irrotational strain field at infinity: this is the Moore–Saffman vortex (Saffman 1992, § 9.3). In the present paper, we will show that non-uniform polygonal vortex patches also constitute steady equilibria of the Euler equations when subjected to strain fields.

Apart from elliptical and weakly deformed polygonal vortex patches whose stability has been studied with classical approaches (Robinson & Saffman 1984; Vladimirov & Il'in 1988; Waleffe 1990; Miyazaki, Imai & Fukumoto 1994; Le Dizès 2000; Eloy & Le Dizès 2001), the three-dimensional stability of the Abrashkin & Yakubovich family of vortices has not to our knowledge been investigated. Technical difficulties arise because of their unsteadiness and the impossibility of expressing their velocity field explicitly in Eulerian form, so that conventional techniques used in stability theory seem inappropriate.

Fortunately, the theory of short-wave instabilities may be applied to such flows described in a Lagrangian representation, as outlined and applied recently to Gerstner's waves (Leblanc 2004). The stability problem is reduced to a set of ordinary differential equations whose main parameter is the distortion matrix of the equilibrium flow. Here, we extend the analysis to the Abrashkin–Yakubovich family of solutions, and also incorporate the effects of background rotation and density stratification.

It is important to note that the present work is restricted to the response of the vortex patches to infinitesimal localized disturbances. Stability with respect to this kind of disturbance does not imply that the flow is linearly stable to all disturbances (in particular with long wavelengths). For instance, Love's instability criterion for Kirchhoff's ellipse cannot be deduced from the local theory.

The paper is organized as follows: the Abrashkin–Yakubovich solution is presented in § 2 and some examples of vortex patches are proposed in § 3. The local stability theory is recalled in § 4 and exact stability criteria are formulated. The stability analysis of vortex patches is presented in § 5, and effects of rotation and stratification are discussed respectively in § 6 and § 7. Results are applied to steady polygonal vortices in § 8. After the concluding part (§ 9), some proofs are presented in the Appendices.

2. The solution of Abrashkin & Yakubovich

In the plane $(O;\hat{\boldsymbol{x}},\hat{\boldsymbol{y}})$, let $\boldsymbol{a}=(a,b)$ be the Lagrangian coordinates of a fluid particle, and $\boldsymbol{X}(t;a,b)=X(t;a,b)\hat{\boldsymbol{x}}+Y(t;a,b)\hat{\boldsymbol{y}}$ its instantaneous position. To describe two-dimensional motions, it is convenient to introduce complex variables. So let

$$\xi = a+\mathrm{i}b, \quad Z(t;\xi,\bar{\xi}) = X(t;a,b)+\mathrm{i}Y(t;a,b)$$

be respectively the complex Lagrangian label and the complex instantaneous position of a fluid particle. In terms of these variables, Abrashkin & Yakubovich proved that $Z(t;\xi,\bar{\xi})$ describes the motion of an incompressible inviscid fluid provided

$$J(\xi,\bar{\xi}) = |\partial_\xi Z|^2-|\partial_{\bar{\xi}} Z|^2, \quad \varGamma(\xi,\bar{\xi}) = 2\mathrm{i}\frac{(\partial_\xi \bar{Z})(\partial_{\bar{\xi}}\dot{Z})-(\partial_{\bar{\xi}}\bar{Z})(\partial_\xi \dot{Z})}{|\partial_\xi Z|^2-|\partial_{\bar{\xi}} Z|^2} \qquad (2.1a,b)$$

are Lagrangian invariant, i.e. independent of time along a fixed trajectory. The dot stands for the material derivative ($\dot{Z}=\partial_t Z$) while the overbar denotes the complex conjugate. In (2.1), $J(\xi,\bar{\xi})$ is the Jacobian determinant of the invertible mapping relating Lagrangian to physical planes, i.e. $J=|\partial(X,Y)/\partial(a,b)|=|\partial(Z,\bar{Z})/\partial(\xi,\bar{\xi})|\neq 0$, while $\varGamma(\xi,\bar{\xi})$ is the local vorticity of fluid particles. Their invariance follows from incompressibility, inviscidness and two-dimensionality.

A class of solutions that satisfy these constraints is (Abrashkin & Yakubovich 1984)

$$Z(t;\xi,\bar{\xi}) = G(\xi)\mathrm{e}^{\mathrm{i}(\lambda+\nu)t}+H(\bar{\xi})\mathrm{e}^{\mathrm{i}(\lambda-\nu)t} \qquad (2.2)$$

where λ and ν are real parameters and the complex analytic functions G and H are arbitrary; the only restriction for the motion to be defined is that $|G'(\xi)|^2 \neq |H'(\bar{\xi})|^2$ which follows from the non-vanishing of the Jacobian (2.1*a*). This class of solutions includes Gerstner's waves as a special case, and the following subclass to which the major part of the paper is devoted:

$$Z(t;\xi,\bar{\xi}) = \xi e^{i\omega t} + H(\bar{\xi}) \quad \text{with} \quad |H'(\bar{\xi})| < 1 \quad \text{and} \quad |\xi| \leqslant 1. \tag{2.3}$$

We assume $\omega > 0$ without loss of generality.† In the trivial case where H is uniform in space ($H' = 0$), the motion is a uniform rotation with angular velocity ω. When H is not uniform, fluid particles still rotate with angular velocity ω along circles with radius $|\xi|$, but the centres of each trajectory located at $H(\bar{\xi})$ differ.

At each instant of time, (2.3) maps the unit disk $|\xi| \leqslant 1$ of the Lagrangian plane onto a deformed surface in the physical plane. The boundary $\mathscr{C}(t)$ of this surface is the mapping of the unit circle $|\xi| = 1$. It is by construction a material contour. Inside or on $\mathscr{C}(t)$, the vorticity of the flow may be computed and is, from (2.1*b*)

$$\Gamma(\xi,\bar{\xi}) = 2\omega/(1 - |H'|^2). \tag{2.4}$$

Thus, vorticity is positive but generally non-uniform in space.

Outside $\mathscr{C}(t)$, Abrashkin & Yakubovich proved that these vortex patches may be matched by a potential flow at rest at infinity. The external potential flow is constructed as follows: the complex velocity field $W = U - iV$ is represented in Eulerian implicit form as

$$W_{ext}(\eta, t) = -i\omega\eta^{-1}e^{-i\omega t}, \tag{2.5}$$

where η is an auxiliary complex parameter such that $|\eta| > 1$ and which is related to the complex coordinate $z = x + iy$ by

$$z = \eta e^{i\omega t} + H(\eta^{-1}). \tag{2.6}$$

Continuity of velocity and pressure across the vortex boundary is ensured (Zeitlin 1991). From (2.5) and (2.6), the complex velocity does not depend on $\bar{z}$ outside $\mathscr{C}(t)$, so that the external flow is potential.

At each instant of time, (2.6) may be recognized as a conformal mapping between the flow exterior to the unit circle in the complex η-plane and the flow exterior to the curve $\mathscr{C}(t)$ in the complex z-plane. According to Yakubovich & Zenkovich (2001), the condition $|H'| < 1$ avoids the existence of singularities in the external potential flow. Finally, since $W_{ext} \sim -i\omega/z$ as $|z| \to \infty$, the Abrashkin–Yakubovich vortex patches behave at infinity as point vortices with circulation $2\pi\omega$.

3. Examples of distorted vortex patches

When H is uniform, (2.3) corresponds to Rankine's circular vortex with uniform vorticity 2ω. When $H'(\bar{\xi}) \neq 0$, the vortex is deformed. The case

$$H(\bar{\xi}) = S\bar{\xi}^{n-1}/(n-1), \tag{3.1}$$

is of interest, where $n \geqslant 2$ is an integer and S a complex number such that $|S| < 1$ to ensure $|H'| < 1$. The phase of S implies only a fixed rotation of the coordinate axes that is irrelevant in the stability analysis. We assume therefore that S is a real number

† More generally, (2.3) may be written as $Z(t;\xi,\bar{\xi}) = A(\xi e^{i\omega t} + H(\bar{\xi}))$ where the positive real number A is a scaling parameter which does not affect the results of the paper.

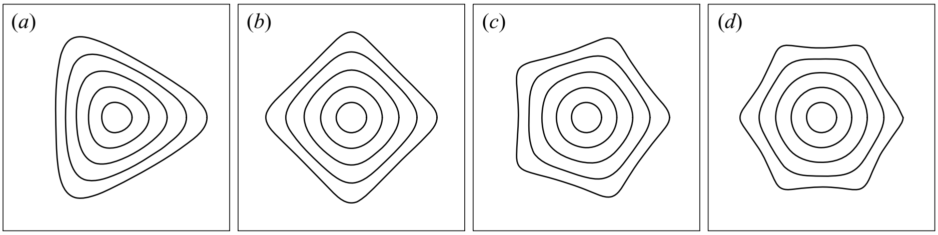

FIGURE 1. Contour lines of vorticity for polygonal vortices (3.1) with $S = 0.4$ and $n = 3$ (a), 4 (b), 5 (c), 6 (d). Vorticity increases from the centre to the boundary. These vortex patches rotate uniformly without change of form in a potential flow at rest at infinity. Rotation may be stopped by imposing a large-scale strain field at infinity (§ 8).

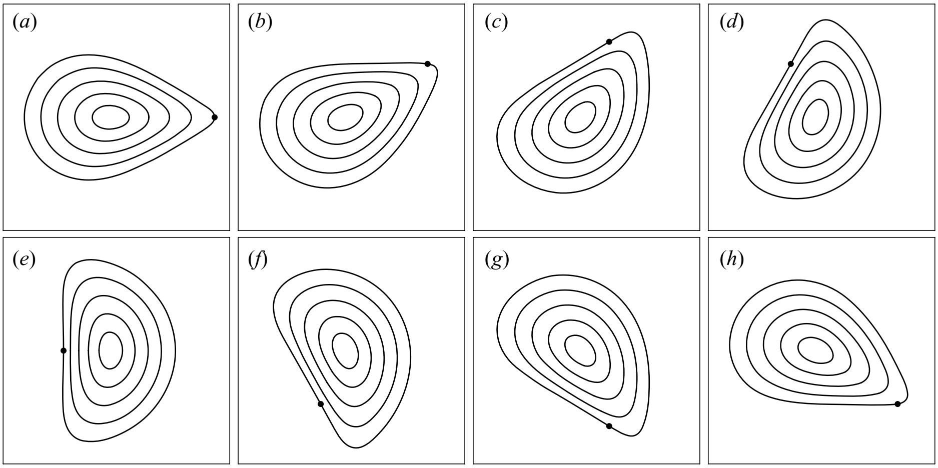

FIGURE 2. Evolution over one period of material contours in the exponential vortex (3.2a) with $S = 0.6$: $\omega t = 0$ (a), $\pi/4$ (b), $\pi/2$ (c), $3\pi/4$ (d), π (e), $5\pi/4$ (f), $3\pi/2$ (g), $7\pi/4$ (h). Contours are instantaneous projections of concentric circles in the Lagrangian ξ-plane. The dot on the vortex boundary represents the material point with maximum vorticity.

such that $0 \leqslant S < 1$. If $n = 2$, the flow corresponds to Kirchhoff's ellipse with uniform vorticity $2\omega/(1 - S^2)$, aspect ratio $(1 + S)/(1 - S)$, and whose axes rotate uniformly at angular velocity $\omega/2$. When $n > 2$, (3.1) represents polygonal vortex patches that rotate without change of form with angular velocity $\omega(1 - 1/n)$.

Except for $n = 2$, vorticity is not uniform: levels of constant vorticity are concentric circles in the Lagrangian plane and hypocycloids in the physical plane. Vorticity increases from the centre of the vortex to its boundary, along which it is constant. Examples of such vortices are plotted on figure 1. Because they are non-uniform, these polygonal vortices differ from those discussed for instance in Saffman (1992, § 9.4). For infinitesimal deformations of the vortex boundaries, we anticipate however that these two branches of solutions are connected (see the end of Appendix C).

Kirchhoff's and polygonal vortices are very specific because they rotate freely without change of form. Generally, for other choices of the function $H(\bar{\xi})$, the vortex contour is deformed continuously with time. Some examples may be found in Abrashkin & Yakubovich (1984) and Yakubovich & Zenkovich (2001). Others are illustrated on figures 2 and 3. They correspond respectively to

$$H(\bar{\xi}) = S \exp(\bar{\xi} - 1) \quad \text{and} \quad H(\bar{\xi}) = S \cos^2 1 \tan \bar{\xi}, \qquad (3.2a, b)$$

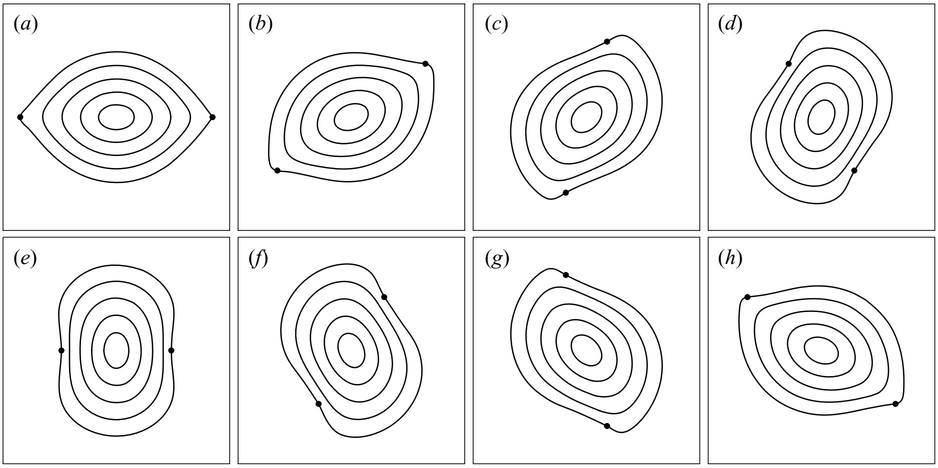

FIGURE 3. Same as figure 2 but for the tangent vortex (3.2*b*). The two dots are vorticity maxima.

where S is chosen real and such that $0 \leqslant S < 1$ for reasons already given. We shall refer to (3.2*a*) and (3.2*b*) respectively as the *exponential* and the *tangent* vortex patches. Unlike the polygonal vortices (3.1), vorticity is no longer constant along the material contours represented on figures 2 and 3, and in particular on their boundary. For instance, the vorticity distribution of the exponential vortex is, from (2.4) and (3.2*a*),

$$\Gamma(\xi, \bar{\xi}) = 2\omega/(1 - S^2 \exp(\xi + \bar{\xi} - 2)).$$

Therefore, levels of constant vorticity are vertical strips in the Lagrangian plane (Reξ constant); the maximum value is reach at the material point $\xi = 1$ of the boundary, and this motion is represented on figure 2. For the tangent vortex, two maxima of vorticity are located at the points $\xi = \pm 1$ represented on figure 3.

In the above examples (3.1) and (3.2*a, b*), the maximum value of the vorticity $\Gamma_{max} = 2\omega/(1 - S^2)$ is finite and reached on the boundary. If $S = 1$, vorticity becomes infinite and cusps appear in the vortex contours. For instance Kirchhoff's ellipse becomes a vortex sheet rotating in a potential flow (Saffman 1992, §9.3). We will not consider such unphysical cases here.

Even with finite vorticity distributions, the physical relevance of these rather exotic vortex patches may be discussed. They are solutions of Euler equations but exhibit a discontinuity of vorticity across their boundary that viscosity will smooth. At low Reynolds number, it is likely that these vortices will relax to axisymmetry by pure diffusion. However at large Reynolds number, dynamics will essentially be inviscid and axisymmetrization of these vortices is an open question. This inviscid mechanism holds for broadly distributed vorticity (Bassom & Gilbert 1998), but Dritschel (1998) has pointed out that "vortices with sufficiently steep edge gradients behave in a radically different way; in particular they can remain non-axisymmetric, apparently indefinitely". Since he considered the dynamics of regularized Kirchhoff ellipses, we can expect that such a conclusion holds for all members of the Abrashkin–Yakubovich solution so that they may represent realistic flows. However, are they stable?

4. General stability criteria

As mentioned in the Introduction, conventional stability techniques cannot be applied to the Abrashkin–Yakubovich solution owing to their unsteadiness and their Lagrangian representation. Thus we restrict our study to infinitesimal short-wavelength disturbances and start with general considerations.

The theory of local instabilities asserts that an equilibrium flow is linearly unstable if it contains at least one unstable trajectory. A trajectory $\boldsymbol{a}$ is said to be unstable if

$$\lim_{t\to\infty} \sup_{\boldsymbol{k}_0 \perp \boldsymbol{v}_0} |\boldsymbol{v}(t;\boldsymbol{a})| = \infty,$$

where the unit vectors $\boldsymbol{k}_0$ and $\boldsymbol{v}_0$ are respectively the initial values of the wave vector $\boldsymbol{k}(t;\boldsymbol{a})$ and the velocity amplitude $\boldsymbol{v}(t;\boldsymbol{a})$ of the disturbance. These are respectively solutions of (Friedlander & Lipton-Lifschitz 2003)

$$\dot{\boldsymbol{k}} = -\mathbf{L}^T \boldsymbol{k}, \quad \dot{\boldsymbol{v}} = (2\boldsymbol{k}\boldsymbol{k}^T/|\boldsymbol{k}|^2 - \mathbf{I})\mathbf{L}\boldsymbol{v}, \tag{4.1a,b}$$

where $\mathbf{L}(t;\boldsymbol{a}) = [\partial \boldsymbol{U}/\partial \boldsymbol{x}](\boldsymbol{X}(t;\boldsymbol{a}),t)$ is the local velocity gradient of the equilibrium flow and $\mathbf{I}$ the identity matrix.

Usually, the equilibrium flow is known in the Eulerian representation through its velocity field $\boldsymbol{U}(\boldsymbol{x},t)$, and the determination of the instantaneous position of fluid particles requires the resolution of $\dot{\boldsymbol{X}} = \boldsymbol{U}(\boldsymbol{X},t)$. This is not necessary here however since trajectories are explicit. Furthermore, both the wave vector $\boldsymbol{k}(t;\boldsymbol{a})$ and the velocity gradient $\mathbf{L}(t;\boldsymbol{a})$ may be computed explicitly from the distortion matrix $\mathbf{F}(t;\boldsymbol{a}) = \partial \boldsymbol{X}/\partial \boldsymbol{a}$ (Leblanc 2004):

$$\boldsymbol{k}(t;\boldsymbol{a}) = (\mathbf{F}_0\mathbf{F}^{-1})^T \boldsymbol{k}_0, \quad \mathbf{L}(t;\boldsymbol{a}) = \dot{\mathbf{F}}\mathbf{F}^{-1}. \tag{4.2a,b}$$

For the Abrashkin–Yakubovich family of solutions (2.2), it is convenient to define the complex distortion matrix $\mathbf{F}_c(t;\xi,\bar{\xi}) = \partial(Z,\bar{Z})/\partial(\xi,\bar{\xi})$ which is given in Appendix A, (A 1). The horizontal part of the distortion matrix $\mathbf{F}_h(t;a,b) = \partial(X,Y)/\partial(a,b)$ may then be computed from the relation (Yakubovich & Zenkovich 2001)

$$\mathbf{F}_c = \mathbf{T}\mathbf{F}_h\mathbf{T}^{-1} \quad \text{where} \quad \mathbf{T} = \frac{\sqrt{2}}{2}\begin{pmatrix} 1 & \mathrm{i} \\ 1 & -\mathrm{i} \end{pmatrix}. \tag{4.3}$$

Therefore from (4.2a,b) both $\boldsymbol{k}$ and $\mathbf{L}$ are explicit. Splitting the wave vector into horizontal and vertical parts as $\boldsymbol{k} = \boldsymbol{k}_h + k_z\hat{\boldsymbol{z}}$, it turns out that $|\boldsymbol{k}_h(t;\boldsymbol{a})|$ is bounded with time, while k_z is constant.

Thus, the only transport equation to solve is (4.1b), or equivalently (Lifschitz 1994)

$$\dot{\boldsymbol{\omega}} = \mathbf{L}\boldsymbol{\omega} + (\boldsymbol{\omega} \times \boldsymbol{k})\boldsymbol{\Gamma} \cdot \boldsymbol{k}/|\boldsymbol{k}|^2, \tag{4.4}$$

where $\boldsymbol{\omega} = \boldsymbol{k} \times \boldsymbol{v}$ is the amplitude of the vorticity disturbance and $\boldsymbol{\Gamma}$ the vorticity of the equilibrium flow. For two-dimensional disturbances ($\boldsymbol{\Gamma} \cdot \boldsymbol{k} = 0$) or along irrotational trajectories, (4.4) becomes $\dot{\boldsymbol{\omega}} = \mathbf{L}\boldsymbol{\omega}$ and admits Cauchy's representation

$$\boldsymbol{\omega}(t;\boldsymbol{a}) = \mathbf{F}\mathbf{F}_0^{-1}\boldsymbol{\omega}_0 \tag{4.5}$$

so that $|\boldsymbol{\omega}(t;\boldsymbol{a})|$ and $|\boldsymbol{v}(t;\boldsymbol{a})|$ are bounded for all time. This proves the first two items of the following proposition:

Local Stability Criteria.

(i) *Two-dimensional disturbances are stable.*

(ii) *Three-dimensional disturbances are stable if* $|H'|^2/|G'|^2 = (\lambda+\nu)/(\lambda-\nu)$.

(iii) *Three-dimensional disturbances are unstable when*

$$\frac{|H'|}{|G'|} > \frac{|2\lambda + \nu|}{|2\lambda - \nu|}. \tag{4.6}$$

The last item is proved for disturbances with vertical wave vector ($\boldsymbol{k}_h = 0$) for which (4.1b) becomes $\dot{\boldsymbol{v}} = -\boldsymbol{L}\boldsymbol{v}$, which may be solved exactly (Appendix A). This is a sufficient condition for instability since it is restricted to that particular orientation of $\boldsymbol{k}$.

These are the most general stability results that we have been able to derive without particularizing the general expression (2.2). For Gerstner's wave, (iii) yields the instability criterion derived in Leblanc (2004) but is unfruitful for vortex patches (2.3). It is therefore necessary to consider disturbances with an oblique wave vector.

5. The instability of distorted vortex patches

As the equilibrium flows under consideration are two-dimensional, Bayly, Holm & Lifschitz (1996) proved that the transport equation (4.4) may be reduced to a second-order ordinary differential equation for the new variable $q = \boldsymbol{\omega}\cdot\hat{\boldsymbol{z}}|\boldsymbol{k}|/|\boldsymbol{k}_h|$:

$$\ddot{q} + Q(t)q = 0, \tag{5.1a}$$

$$Q(t) = -k_z^2\left(\frac{\boldsymbol{k}_h^T(\dot{\boldsymbol{L}} + \boldsymbol{L}\boldsymbol{L} - 3\boldsymbol{L}\boldsymbol{L}^T)\boldsymbol{k}_h}{|\boldsymbol{k}_h|^2|\boldsymbol{k}|^2} + \frac{\left(4|\boldsymbol{k}|^2 - k_z^2\right)\left(\boldsymbol{k}_h^T\boldsymbol{L}\boldsymbol{k}_h\right)^2}{|\boldsymbol{k}_h|^4|\boldsymbol{k}|^4}\right). \tag{5.1b}$$

The flow is unstable if $|q(t)|$ grows without bound along some trajectory. (Dependence with respect to the Lagrangian label is now implicit for brevity.)

For the vortex patches (2.3), it may be shown after some algebra that the coefficient Q in (5.1) has the following explicit dependence: $Q(t;\omega,\delta,\vartheta,\gamma-2\varphi)$. Here, δ and γ are respectively the modulus and argument of $H'(\bar{\xi})$, while φ and ϑ are the angles characterizing the initial orientation of the wave vector $\boldsymbol{k}_0 = (\cos\varphi\sin\vartheta, \sin\varphi\sin\vartheta, \cos\vartheta)^T$.

It turns out that Q is periodic in time with period $2\pi/\omega$, so that (5.1) is a Hill's equation. Furthermore, the potential Q is invariant for the following transformations $\vartheta \to -\vartheta$, $\vartheta \to \pi - \vartheta$, and $\varphi \to \varphi + \pi$. Since the orientation of the initial wave vector $\boldsymbol{k}_0$ is left free, we choose in the rest of the paper and for simplicity of the presentation φ such that $\gamma - 2\varphi = \pi/2$. Other values of φ do not qualitatively affect the results given below.

The parameters $\delta \in [0;1[$ and $\vartheta \in [0;\pi/2]$ are the most important of the present problem. Recall that $\delta = |H'|$ characterizes the local deformation experienced by a fluid particle and is generally not uniform in the vortex patch; recall also that if $\delta = 0$ everywhere, the flow is a circular Rankine's vortex. ϑ is the angle between the initial wave vector and the vertical axis; the disturbance is two-dimensional if $\vartheta = \pi/2$ and three-dimensional otherwise.

First, we consider the stability of weakly distorted flows, i.e. $\delta \ll 1$. For the examples considered in (3.1) and (3.2a,b), it corresponds to $S \ll 1$. At first order in δ, (5.1) gives

$$\ddot{q} + \omega^2(a_0 + 2\delta a_1 \sin\omega t)q = 0. \tag{5.2}$$

This is a Mathieu equation with coefficients:

$$a_0 = 4\cos^2\vartheta, \quad a_1 = \left(\tfrac{5}{2} + 4\sin^2\vartheta\right)\cos^2\vartheta. \tag{5.3}$$

When $\delta \ll 1$, solutions of (5.2) are bounded except in the vicinity of resonances defined by $a_0 = \frac{1}{4}j^2$ where j is a positive integer. Resonant solutions are exponentially growing

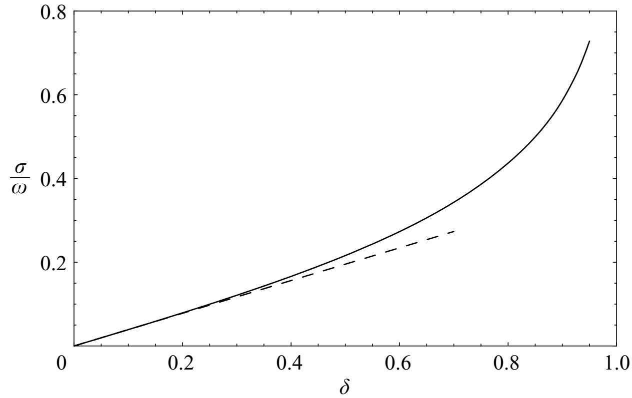

FIGURE 4. Computed dimensionless growth rate σ/ω (maximized over all possible orientations of the wave vector) for the Abrashkin–Yakubovich vortices (2.3) as a function of the local deformation $\delta = |H'|$, without background rotation nor density stratification. The dashed line with slope 25/64 corresponds to the small-δ asymptotics.

with growth rate of order δ^j. By a perturbation analysis, the maximum growth rate associated with the first-order resonance ($j = 1$) is $\sigma = \delta\omega a_1$ (Bender & Orszag 1978, § 11.4).

From (5.3), first-order resonance occurs when $\cos\vartheta = \frac{1}{4}$ and the growth rate of the corresponding solution is $\sigma = \frac{25}{64}\omega\delta$. Since $\delta = |H'|$, we can conclude that any weakly deformed vortex column of the form (2.3) is unstable to three-dimensional localized disturbances. For the examples (3.1) and (3.2*a, b*), the maximum value of the asymptotic growth rate is

$$\sigma_{max} = \frac{25}{64}\omega S \quad \text{with} \quad S \ll 1.$$

Thus, one recovers the results of Vladimirov & Il'in (1988) and Le Dizès (2000) for Kirchchoff or polygonal vortices, but surprisingly this result holds for the full family of vortices by replacing S by $|H'|_{max}$. An explanation will be given at the end of the paper in § 9.

For strong deformations, Mathieu's equation (5.2) is no longer valid and (5.1) requires a numerical integration. Since $Q(t)$ is periodic, this is achieved with Floquet's theory (Bender & Orszag 1978, § 11.4). Results reported on figure 4 show that *the Abrashkin–Yakubovich family of vortices is unstable if* $H'(\bar{\xi}) \neq 0$ *somewhere.* Rankine's vortex is therefore the only stable member of that family.

Figure 4 also shows that the growth rate is enhanced by distortion. Since $\delta = |H'|$, the growth of the disturbances is not uniform in the vortex. Furthermore, since vorticity (2.4) is an increasing function of $|H'|$, the most unstable regions are those where vorticity is maximum. As an example, the most dangerous instabilities are located along the boundary of the polygonal vortices (3.1) represented on figure 1. For (3.2*a, b*), the material points represented on figures 2 and 3 carry the most unstable disturbances.

6. Effect of background rotation

A particular case of the Abrashkin–Yakubovich solution (2.2) is

$$Z(t; \xi, \bar{\xi}) = (\xi e^{i\omega t} + H(\bar{\xi}))e^{i\Omega t} \quad \text{with} \quad |H'(\bar{\xi})| < 1 \quad \text{and} \quad |\xi| \leqslant 1. \tag{6.1}$$

The motion thus defined is (2.3) with a uniform rotation around the vertical axis $(O\hat{z})$ at angular velocity Ω, assumed constant. Therefore, (2.3) may be seen as the relative position of a fluid particle in the frame rotating at Ω, and (6.1) its absolute position with respect to the inertial frame $(O; \hat{x}, \hat{y}, \hat{z})$. The exterior flows of the vortex patches constructed in § 2 are still irrotational when viewed from the rotating frame, but have uniform vorticity 2Ω in the inertial frame.

The consequence is that the direct stability analysis of (6.1) is equivalent to the stability of (2.3) in the rotating frame. Therefore, the method presented in the previous section may be applied directly to (6.1), provided the complex distortion matrix $\boldsymbol{F}_c$ is computed from (6.1).

Explicit calculation of the vorticity associated with (6.1) yields

$$\Gamma(\xi, \bar{\xi}) = 2\Omega + 2\omega/(1 - |H'|^2). \tag{6.2}$$

This is the absolute vorticity of the motion which is related to the relative vorticity (2.4) through the usual relation: $\Gamma_{abs} = 2\Omega + \Gamma_{rel}$. Recalling that ω is the angular velocity of a fluid particle in its motion relative to the rotating frame, it is useful to introduce the following dimensionless parameter:

$$f = \Omega/\omega.$$

This is the inverse of a Rossby number. Background rotation is cyclonic if $f > 0$ and anticyclonic if $f < 0$.

For weak distortions ($\delta = |H'| \ll 1$), the Mathieu equation (5.2) has coefficients

$$a_0 = 4(1+f)^2 \cos^2\vartheta, \quad a_1 = \left(\left(\tfrac{5}{2} + 2f\right) + 4(1+f)^2 \sin^2\vartheta\right)\cos^2\vartheta.$$

Since $0 \leqslant \cos^2\vartheta \leqslant 1$, the first-order resonance ($a_0 = \frac{1}{4}$) occurs only when

$$|1 + f| \geqslant \tfrac{1}{4}, \tag{6.3}$$

which is either when $f \leqslant -\frac{5}{4}$ or when $f \geqslant -\frac{3}{4}$. Inside these regions, resonant solutions grow exponentially with dimensionless growth rate

$$\frac{\sigma}{\omega} = \frac{\delta}{64}\left(\frac{5+4f}{1+f}\right)^2. \tag{6.4}$$

Therefore when $\delta \ll 1$, Abrashkin–Yakubovich vortex patches are stable in a rotating frame only for anticyclonic rotations such that $-\frac{5}{4} \leqslant f \leqslant -\frac{3}{4}$.

This stable region is centred around $f = -1$ from which it may be concluded from (6.2) with $\delta \ll 1$, that the absolute vorticity of the flow is close to zero. In fact for strong deformations, trajectories with zero absolute vorticity $f + 1/(1 - \delta^2) = 0$ are stable as a consequence of item (ii) of the criteria formulated in § 4. This is an extension of the well-known result that the elliptical instability is stabilized in a rotating frame at zero absolute vorticity (Craik 1989; Cambon *et al.* 1994).

For strong deformations, the criterion (4.6) for disturbances with vertical wave vectors predicts instability if

$$\delta > |3 + 4f|/|1 + 4f|. \tag{6.5}$$

Inside that region, the dimensionless growth rate is given by

$$\frac{\sigma}{\omega} = \left(\frac{\delta^2(1+4f)^2 - (3+4f)^2}{4(1-\delta^2)}\right)^{1/2}. \tag{6.6}$$

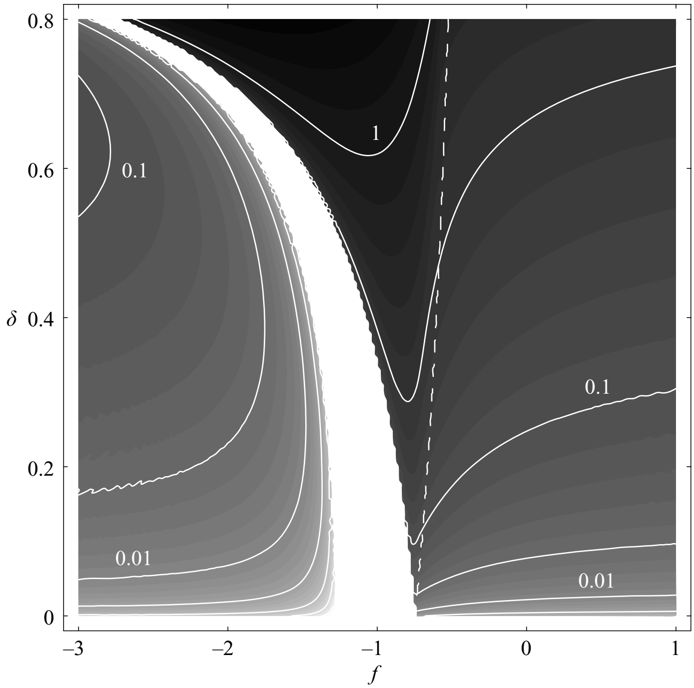

FIGURE 5. Instability map for rotating vortex patches (6.1) in a non-stratified flow. Contour lines of the computed maximum dimensionless growth rate σ/ω as a function of the vortex deformation $\delta = |H'|$ and the rotation parameter $f = \Omega/\omega$. The levels of grey are scaled in decimal logarithm. The white region is stable. The region delimited by dashed lines which includes the contour $\sigma/\omega = 1$ (the left-hand line coincides with the right-hand edge of the white region) is the region in which disturbances with vertical wave vectors are unstable.

For all other values of the parameters, the resolution of the problem requires the numerical integration of Hill's equation (5.1). Formulae (6.4) and (6.6) provide useful checks for the accuracy of the numerical computations. Results are represented on figure 5 where the growth rate maximized over all possible orientations of the initial wave vector is plotted as a function of the parameters (f, δ). For $f = 0$ (no background rotation), the vortices (2.3) are unstable for any non-zero deformation, as already mentioned. While cyclonic rotations ($f > 0$) are always unstable, anticyclonic ones may be stabilizing.

The (f, δ)-plane may be divided into four regions that are represented on figure 6(*a*): the region T defined by (6.5) in which disturbances with transverse (vertical) and eventually oblique wave vectors are unstable; the two regions I in which only disturbances with oblique wave vector are unstable; and the stable region S which includes trajectories with zero absolute vorticity. Figure 5 shows that the largest growth rates are reached in region T. A careful inspection of the results shows that the stable region is bounded by two curves along which disturbances with transverse wave vector ($\boldsymbol{k}_h = 0$) are stable but periodic with period π, and that cross the $\delta = 0$ axis respectively at $f = -\frac{5}{4}$ and $f = -\frac{3}{4}$ as predicted for the first resonance of Mathieu equation. It may be shown that such curves are defined respectively by $\delta_2(f)$ and $\delta_0(f)$, where

$$\delta_m(f) = \left(\frac{(3+4f)^2 - m^2}{(1+4f)^2 - m^2}\right)^{1/2}. \tag{6.7}$$

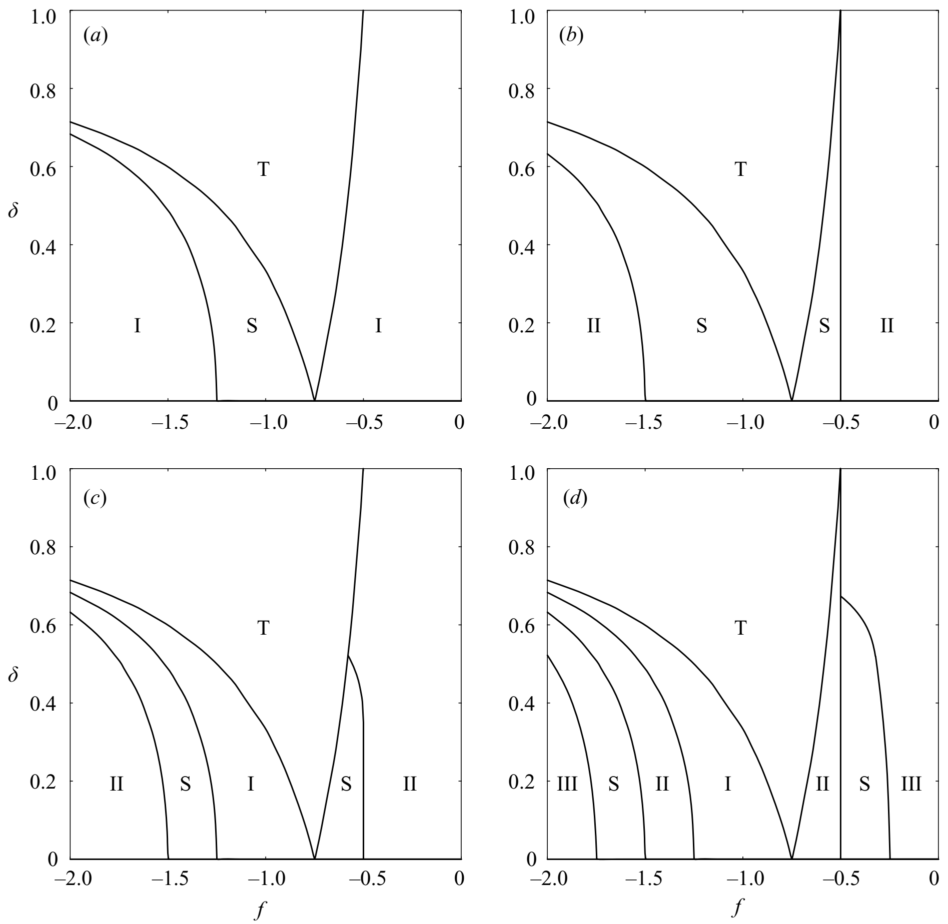

FIGURE 6. Stability diagrams for vortex patches in a rotating stratified flow for $s = N/\omega < \frac{1}{2}$ (*a*), $s = \frac{1}{2}$ (*b*), $s = \frac{3}{4}$ (*c*), $s = \frac{5}{4}$ (*d*). Regions labelled by S are stable; those by T are unstable with respect to disturbances with transverse (vertical) wave vector. Resonances of order 1, 2 and 3 develop respectively in regions I, II and III.

Note that the curve corresponding to zero absolute vorticity is given by $m = 1$ and is included into the stable region $\delta_2(f) \leqslant \delta \leqslant \delta_0(f)$. To conclude, *the Abrashkin–Yakubovich vortices are stabilized by rotation if* $f \leqslant -\frac{3}{4}$ *and if for any point*

$$\left(\frac{(3+4f)^2-4}{(1+4f)^2-4}\right)^{1/2} \leqslant |H'| \leqslant \frac{3+4f}{1+4f}. \tag{6.8}$$

It is important to emphasize from these results that even strongly distorted vortices may be stabilized for anticyclonic rotations. For instance, it is always possible to find a rotating frame in which a given Kirchhoff ellipse with arbitrary large aspect ratio is stable. Non-uniform vortices such as those given by (3.1) or (3.2*a,b*) are stable in the region defined by $-\frac{5}{4} \leqslant f \leqslant -\frac{3}{4}$ providing that $S \leqslant (3+4f)/(1+4f)$. If $f = -\frac{5}{4}$ for instance, stable vortices correspond to $S \leqslant \frac{1}{2}$ (for Kirchhoff ellipses, the aspect ratio must be less than or equal to 3).

7. Effect of density stratification

We now study the effects of uniform stable density stratification along the vertical direction $\hat{z}$. Under the Boussinesq approximation, it is shown in Appendix B that the transport equations may be reduced to

$$\ddot{q} + \left(Q(t) + N^2 \frac{|\boldsymbol{k}_h(t)|^2}{|\boldsymbol{k}(t)|^2} \right) q = 0, \tag{7.1}$$

where N is the Brunt–Väisälä frequency, and $Q(t)$ the potential defined in (5.1). It is convenient here to introduce the dimensionless stratification parameter

$$s = N/\omega,$$

which is the inverse of a horizontal Froude number.

When the vortex distortion is weak, the Mathieu equation (5.2) has coefficients

$$a_0 = 4(1+f)^2 \cos^2\vartheta + s^2 \sin^2\vartheta, \quad a_1 = (\tfrac{5}{2} + 2f + (4(1+f)^2 - s^2)\sin^2\vartheta)\cos^2\vartheta.$$

At first order, instability occurs when $a_0 = \frac{1}{4}$. Since $0 \leqslant \cos^2\vartheta \leqslant 1$ and $s^2 \geqslant 0$, the conditions for parametric resonance become, in the presence of (stable) stratification†,

$$\left(s \leqslant \tfrac{1}{2} \text{ and } |1+f| \geqslant \tfrac{1}{4}\right) \quad \text{or} \quad \left(s \geqslant \tfrac{1}{2} \text{ and } |1+f| \leqslant \tfrac{1}{4}\right). \tag{7.2}$$

Inside these regions, the dimensionless growth rate of short-wave instabilities is

$$\frac{\sigma}{\omega} = \frac{\delta(5+4f)^2(1-4s^2)}{64(1+f)^2 - 16s^2}.$$

Thus, for low stratification ($s \leqslant \frac{1}{2}$), the mechanism of stabilization of the vortex patches for zero absolute vorticity still operates, but for larger stratifications ($s \geqslant \frac{1}{2}$) stability and instability regions interchange. However, higher-order resonances corresponding to $a_0 = \frac{1}{4}j^2$ with $j \geqslant 2$ may arise in regions that are stable with respect to the first-order resonance $j = 1$. For instance, if $s = \frac{1}{2}$ and $\delta \ll 1$, the first-order resonance disappears whereas the second-order one ($j = 2$) develops if $f \leqslant -\frac{3}{2}$ or $f \geqslant -\frac{1}{2}$ (region II in figure 6*b*). If $\frac{1}{2} < s < 1$ and $\delta \ll 1$, this latter resonance is still present while the first-order resonance reappears now for $-\frac{5}{4} \leqslant f \leqslant -\frac{3}{4}$ (region I in figure 6*c*). If $1 < s < \frac{3}{2}$ and $\delta \ll 1$, the second-order resonance is shifted, and the third-order one appears (figure 6*d*), and so on.

These higher-order resonances are very difficult to detect numerically because their growth rate is of order δ^j as $\delta \ll 1$. Fortunately, as δ is finite but small enough, we have observed that the boundaries of the regions in which they develop in the (f, δ)-plane are given by the curves defined by (6.7), on which disturbances with vertical wave vector are stable. This provides useful guides for numerical computations of (7.1) for finite deformations. Results are presented on figure 6.

At first, the region T defined by (6.5) containing disturbances with transverse wave vector remains for any stratification since these kinds of disturbance are not affected by buoyancy (see Appendix B). Inside that region short-wave disturbances are the most amplified, their growth rate being equal to (6.6) (except very near the bounds of T). For weak stratification $0 < s < \frac{1}{2}$, we have observed that the first-order resonance develops in the same regions (I) as in the homogeneous case, although with weaker

† Reversed stratification $s^2 < 0$ is unstable as there always exists ϑ such that $a_0 < 0$.

growth rate (figure 6*a*). The stable region S remains unchanged. Thus, if $s < 1$ and $f \leqslant -\frac{3}{4}$, Abrashkin–Yakubovich vortices are stable provided (6.8) holds everywhere.

If $s = \frac{1}{2}$ (figure 6*b*), we observed numerically that the first-order resonance disappears, even for strong deformations, and that the second-order resonance develops in two regions (II) bounded by curves defined respectively by $\delta_3(f)$ and $f = -\frac{1}{2}$. There are now two regions of stability defined respectively by

$$\left(f \leqslant -\tfrac{3}{4} \text{ and } \delta_3(f) \leqslant |H'| \leqslant \delta_0(f)\right) \quad \text{and} \quad \left(-\tfrac{3}{4} \leqslant f \leqslant -\tfrac{1}{2} \text{ and } |H'| \leqslant \delta_0(f)\right).$$

Surprising, any distorted vortex patch is stable if $s = \frac{1}{2}$ and $f = -\frac{1}{2}$.

If $\frac{1}{2} < s < 1$ (figure 6*c*), the bounds between the various regions are still given by the functions $\delta_m(f)$ if $f \leqslant -\frac{3}{4}$. However, for $-\frac{3}{4} \leqslant f \leqslant -\frac{1}{2}$, we can observe by comparing figures 6(*b*) and 6(*c*) that the stable region is smaller. In fact, a new instability region that depends on the magnitude of stratification arises. For instance if $s = 0.75$, the boundary of that region starts at the point $(f, \delta) \approx (-0.5, 0.35)$ and crosses the region T at the point $(f, \delta) \approx (-0.58, 0.52)$. We have not been able to obtain an expression for that curve because unlike the other curves separating stable and unstable regions, this is not characterized by transverse wave vectors.

Thus, unless the deformation is small enough, it seems not to be possible to give a systematic description of the stability bounds if $s > \frac{1}{2}$. Another example is presented for $s = 1.25$ on figure 6(*d*). Recall however that resonances of order greater than one are very weak and therefore sensitive to viscous damping. Thus, if $s > \frac{1}{2}$, the qualitative picture of instability would be the joining of regions T and I of figures 6(*c*) or 6(*d*), regions II and III being almost stable.

8. Application to steady polygonal equilibria

We finally consider the following member of the Abrashkin–Yakubovich family:

$$Z(t;\xi,\bar{\xi}) = (\xi + S\bar{\xi}^{n-1}\mathrm{e}^{-\mathrm{i}\omega t})\mathrm{e}^{\mathrm{i}\omega t/n}/(n-1) \tag{8.1}$$

where $0 \leqslant S < 1$ and $|\xi| \leqslant 1$. It is clearly a particular case of (2.2), and more precisely of (6.1) where $H(\bar{\xi})$ is given by (3.1) and $\Omega = -\omega(1 - 1/n)$. Since we have seen in § 3 that (2.3) with (3.1) correspond to polygonal vortices that rotate without change of form with angular velocity $\omega(1 - 1/n)$, then (8.1) describes steady polygonal equilibria. An alternative proof is given in Appendix C.

This solution is of particular interest because it is possible to construct outside the vortex a steady potential flow that behaves as a multipolar strain field at infinity (Appendix C). This exact solution is therefore a generalization of the Moore–Saffman elliptical vortex. From (6.2), the vorticity distribution of (8.1) may be computed: it is again non-uniform if $n > 2$ and is still represented by figure 1 where now the contours also coincide with streamlines. When $S \ll 1$ (weak deformations), vorticity is uniform to a first approximation ($\Gamma = 2\omega/n$), while the stream function is given in polar coordinate by (C 5). For $S \ll 1$, the flow therefore corresponds to the multipolar solution considered by Le Dizès (2000) and Eloy & Le Dizès (2001).

Since it is a particular case of (6.1), the stability of the steady polygonal flow (8.1) may be easily characterized from the results obtained in the previous sections by simply replacing f by $1/n - 1$. For instance without stratification, the stability condition (6.8) shows that steady elliptical ($n = 2$), triangular ($n = 3$) and square ($n = 4$) vortices are unstable for any $0 < S < 1$, while higher-order equilibria are unstable only if the deformation is large enough. More precisely, (8.1) with $n \geqslant 5$ is stable if

$$S < (n-4)/(3n-4). \tag{8.2}$$

In the homogeneous case, but for weak deformations $S \ll 1$, the asymptotic formula (6.4) for the growth rate may be directly applied to (8.1) with $f = 1/n - 1$ and $\delta = S|\xi|^{n-2}$. The condition for resonance (6.3) is $n \leqslant 4$, in agreement with Eloy & Le Dizès (2001), and the maximum asymptotic growth rate is reached on $|\xi| = 1$:

$$\sigma_{max} = \tfrac{1}{64}(n+4)^2 \omega S.$$

For $n = 2$, one finds the well-known $\frac{9}{16}$ value of Waleffe (1990) for the elliptical instability (here, when $S \ll 1$, the strain rate and vorticity of the flow are respectively ωS and ω). For $n = 3$ and 4, formula (50) in Le Dizès (2000) is also recovered. In the presence of low stratification ($s = N/\omega < \frac{1}{2}$), the conclusions above still hold, the maximum asymptotic growth rate for weak deformations ($S \ll 1$) being replaced by

$$\sigma_{max} = \frac{(n+4)^2(1-4s^2)}{16(4-n^2s^2)}\omega S. \tag{8.3}$$

If $s = \frac{1}{2}$, elliptical vortices are stable for any ellipticity, triangular vortices are stable if $S < \frac{1}{5}$, square vortices are all unstable, and the other ones are stable if (8.2) holds. In fact, square vortices ($n = 4$) are always unstable, for any stratification. If $s > \frac{1}{2}$, it can be deduced from (7.2) that the first-order resonance occurs when $n \geqslant 4$ with growth rate (8.3). This shows that while weakly deformed polygonal vortices with $n \geqslant 5$ are stable in a homogeneous fluid in agreement with (8.2), they become unstable if stratification is strong enough ($s > \frac{1}{2}$). On the contrary, the first-order resonance in steady elliptical or triangular equilibria is stabilized by stratification. Such a mechanism was discovered by Miyazaki & Fukumoto (1992) in the elliptical case. Higher-order resonances arise if $s > 1$ however.

Finally, if an additional background rotation is superimposed, that is if (8.1) corresponds to steady motion relative to a frame which rotates at angular velocity Ω with respect to an inertial frame, the asymptotic results may be deduced from (6.4) and (8.3) by replacing f in these formulae by $f + 1 - 1/n$. When $n = 2$, we would recover the stability characteristics of an elliptical vortex in a rotating stratified flow (Miyazaki 1993; Kerswell 2002; Leblanc 2003), while for $n \geqslant 3$, the results obtained by Le Dizès (2000) would be extended to a stratified flow.

9. Summary and conclusion

We first summarize the main results of the paper. Several exact stability criteria have been expressed in §4 for the Abrashkin–Yakubovich class of solutions (2.2). Among them, the instability criterion for Gerstner's wave derived previously has been extended.

The rest of the paper has been devoted to the family of non-uniform distorted vortex patches described by $Z(t, \xi, \bar{\xi}) = \xi e^{i\omega t} + H(\bar{\xi})$ and that evolve freely in a potential flow at rest at infinity. We found that:

(i) Apart from Rankine vortices, in a homogeneous fluid they are unstable to three-dimensional short-wave disturbances. Two-dimensional ones are stable.

(ii) In a rotating frame, short-wave disturbances are stabilized for anticyclonic rotations ($f \leqslant -\frac{3}{4}$) if (6.8) holds everywhere in the vortex. The same conclusion holds in a rotating stratified flow if $s < \frac{1}{2}$.

(iii) If $s = \frac{1}{2}$ and $f = -\frac{1}{2}$, no short-wave instabilities have been detected.

These results, valid for any member of the family of vortices, have been applied in § 8 to steady polygonal equilibria (8.1) which we have proved can be surrounded by a potential strain field. We found in particular that square vortices are always unstable, that elliptical and triangular vortices are unstable if $s < \frac{1}{2}$, the other ones being stable if (8.2) holds. For larger stratification ($s > \frac{1}{2}$), we found that polygonal vortices with $n > 4$ are unstable, while the first-order resonance is stabilized in elliptical and triangular equilibria.

We conclude with an explanation of the instability mechanism described in this paper. Recall that when $H(\bar{\xi}) = S\bar{\xi}$, the Abrashkin–Yakubovich solution corresponds to Kirchhoff's freely rotating ellipse. In that case, vorticity and strain are uniform inside the ellipse, and the local stability analysis is mathematically equivalent to the stability of an unbounded flow with elliptical streamlines in a frame which rotates with angular velocity $\omega/2$. In fact, for distorted vortex patches described by an arbitrary analytic function $H(\bar{\xi})$, an analogy with the elliptical instability may be made, although vorticity and local strain are not uniform inside the vortex. Indeed, the local velocity gradient of a fluid particle may be computed in explicit form. Split into symmetric and antisymmetric part, is (without background rotation)

$$\boldsymbol{L}(t;\xi,\bar{\xi}) = \frac{\omega\delta}{1-\delta^2}\begin{pmatrix} \sin(\omega t+\gamma) & -\cos(\omega t+\gamma) \\ -\cos(\omega t+\gamma) & -\sin(\omega t+\gamma)\end{pmatrix} + \frac{\omega}{1-\delta^2}\begin{pmatrix} 0 & -1 \\ 1 & 0\end{pmatrix},$$

where δ and γ are respectively the modulus and the argument of $H'(\bar{\xi})$, varying from one trajectory to another. The symmetric part shows that each fluid particle experiences a local strain field that rotates with angular velocity $\omega/2$.

However, the local stability analysis considers each trajectory individually, so that the stability of each trajectory of the solution of Abrashkin & Yakubovich is in fact equivalent to the stability analysis of a rotating elliptical flow with aspect ratio $(1+\delta)/(1-\delta)$. Thus, elliptical instability operates in the Abrashkin–Yakubovich vortices though their shape differs from ellipses. This illustrates once more the universality of this mechanism.

This work has benefited from the support of Ministère de la Recherche with Action Concertée Incitative (ACI) "Prévention des catastrophes naturelles" (supervised by Jan-Bert Flór) and ACI "Jeunes chercheuses et jeunes chercheurs". We acknowledge the referees for their constructive criticism.

Appendix A. Proof of the instability criterion

We prove that the solution (2.2) is unstable if inequality (6.5) holds somewhere. For this, we consider disturbances whose wave vector is perpendicular to the plane of the flow ($\boldsymbol{k}_h = 0$), for which (4.1*b*) becomes $\dot{\boldsymbol{v}} = -\boldsymbol{L}\boldsymbol{v}$.

The complex Jacobian matrix $\boldsymbol{F}_c = \partial(Z,\bar{Z})/\partial(\xi,\bar{\xi})$ is

$$\boldsymbol{F}_c(t) = \begin{pmatrix} G'\mathrm{e}^{\mathrm{i}(\lambda+\nu)t} & H'\mathrm{e}^{\mathrm{i}(\lambda-\nu)t} \\ \overline{H'}\mathrm{e}^{-\mathrm{i}(\lambda-\nu)t} & \overline{G'}\mathrm{e}^{-\mathrm{i}(\lambda+\nu)t}\end{pmatrix}, \tag{A 1}$$

where for brevity $\overline{G'} = \overline{G'(\xi)}$ and $\overline{H'} = \overline{H'(\bar{\xi})}$. Recall that $\boldsymbol{F}_c(t)$ and $\boldsymbol{F}_h(t)$ are related by (4.3), and that $\boldsymbol{L}(t)$ and $\boldsymbol{F}(t)$ are related by $\dot{\boldsymbol{F}} = \boldsymbol{L}\boldsymbol{F}$, then the complex velocity gradient defined by $\boldsymbol{L}_c = \boldsymbol{T}\boldsymbol{L}_h\boldsymbol{T}^{-1}$ is related to $\boldsymbol{F}_c$ by

$$\dot{\boldsymbol{F}}_c = \boldsymbol{L}_c\boldsymbol{F}_c. \tag{A 2}$$

If we also introduce the complex vector $\boldsymbol{v}_c = \boldsymbol{T}\boldsymbol{v}_h$ where $\boldsymbol{v}_h(t)$ is the horizontal part of the velocity disturbance, then $\boldsymbol{v}_c(t)$ is governed for vertical wave vectors by

$$\dot{\boldsymbol{v}}_c = -\boldsymbol{L}_c \boldsymbol{v}_c. \tag{A 3}$$

Now, from (A 1) and (A 2), explicit computation yields

$$\boldsymbol{L}_c(t) = \frac{\mathrm{i}}{J}\begin{pmatrix} \nu I + \lambda J & -2\nu G' H' \mathrm{e}^{2\mathrm{i}\lambda t} \\ 2\nu \overline{G' H'} \mathrm{e}^{-2\mathrm{i}\lambda t} & -\nu I - \lambda J \end{pmatrix}, \tag{A 4}$$

where $I = |G'|^2 + |H'|^2$ and $J = |G'|^2 - |H'|^2$.

System (A 3) with (A 4) has periodic coefficients but may be transformed into a system with constant coefficients by introducing the following matrices:

$$\boldsymbol{R} = \begin{pmatrix} \mathrm{i}\lambda & 0 \\ 0 & -\mathrm{i}\lambda \end{pmatrix} \quad \text{and} \quad \boldsymbol{P}(t) = \mathrm{e}^{t\boldsymbol{R}} = \begin{pmatrix} \mathrm{e}^{\mathrm{i}\lambda t} & 0 \\ 0 & \mathrm{e}^{-\mathrm{i}\lambda t} \end{pmatrix}.$$

Since $\dot{\boldsymbol{P}} = \boldsymbol{R}\boldsymbol{P}$ and $\boldsymbol{P}^{-1}\boldsymbol{R}\boldsymbol{P} = \boldsymbol{R}$, then the new variable $\boldsymbol{w} = \boldsymbol{P}^{-1}\boldsymbol{v}_c$ is, from (A 3), governed by $\dot{\boldsymbol{w}} = -\boldsymbol{M}\boldsymbol{w}$ where $\boldsymbol{M} = \boldsymbol{P}^{-1}\boldsymbol{L}_c\boldsymbol{P} + \boldsymbol{R}$. Explicit computations give

$$\boldsymbol{M} = \frac{\mathrm{i}}{J}\begin{pmatrix} \nu I + 2\lambda J & -2\nu G' H' \\ 2\nu \overline{G' H'} & -\nu I - 2\lambda J \end{pmatrix},$$

which is, as required, time independent. Eigenvalues of $\boldsymbol{M}$ satisfy $\sigma^2 = -4\lambda^2 - \nu^2 - 4\lambda\nu I/J$. Disturbances grow exponentially if $\sigma^2 > 0$ and the flow (2.2) is unstable if for some point $(\xi, \bar{\xi})$ in the complex Lagrangian plane, inequality (6.5) holds.

Appendix B. Derivation of Hill's equation

In the Boussinesq approximation, equations governing the motion of an inviscid stratified flow are given by (LeBlond & Mysak 1978, § 1.5)

$$\mathrm{D}\boldsymbol{u}/\mathrm{D}t + \nabla\varpi = -b\hat{\boldsymbol{z}}, \quad \mathrm{D}b/\mathrm{D}t = N^2\boldsymbol{u}\cdot\hat{\boldsymbol{z}}, \quad \operatorname{div}\boldsymbol{u} = 0,$$

where $b(\boldsymbol{x}, t)$ is the buoyancy field, and N is the Brunt–Väisälä frequency. Stratification is assumed stable and uniform (N real and constant).

Let $\boldsymbol{U}(\boldsymbol{x}, t)$ and $B(\boldsymbol{x}, t)$ be the velocity and buoyancy fields of an exact solution of the Boussinesq equations. To study the response of that flow to an initially localized disturbance, we linearize the equations about the equilibrium solution, and look for a perturbation of the form $(\boldsymbol{u}, \varpi, b) = (\boldsymbol{v}, 0, \varrho)\mathrm{e}^{\mathrm{i}\phi/\varepsilon} + O(\varepsilon)$, where $0 < \varepsilon \ll 1$. Following the formal asymptotic procedure outlined by Lifschitz & Hameiri (1991), it can be shown that while the wave vector $\boldsymbol{k} = \nabla\phi$ is still governed by (4.1*a*), the velocity and buoyancy amplitudes $(\boldsymbol{v}, \varrho)$ of the disturbance are governed by the following transport equations (see also Friedlander 2001):

$$\dot{\boldsymbol{v}} = (2\boldsymbol{k}\boldsymbol{k}^T/|\boldsymbol{k}|^2 - \boldsymbol{I})\boldsymbol{L}\boldsymbol{v} + (\boldsymbol{k}\boldsymbol{k}^T/|\boldsymbol{k}|^2 - \boldsymbol{I})\varrho\hat{\boldsymbol{z}}, \quad \dot{\varrho} = (N^2\hat{\boldsymbol{z}} - \nabla B)\cdot\boldsymbol{v}. \tag{B 1a, b}$$

Any two-dimensional equilibrium solution of the Euler equations in the horizontal plane is also a solution of the Boussinesq equation with zero buoyancy. Thus the Abrashkin–Yakubovich solutions (2.3) and (6.1) may represent vertical vortex columns that evolve in a stably stratified flow. We now show how to reduce the transport equations (B 1) to a second-order differential equation of the form (7.1). The construction follows that of Bayly *et al.* (1996), but density stratification requires additional arguments.

In the presence of stratification, Lifschitz's equation (4.4) is

$$\dot{\boldsymbol{\omega}} = \boldsymbol{L}\boldsymbol{\omega} + (\boldsymbol{\omega} \times \boldsymbol{k})\boldsymbol{\Gamma} \cdot \boldsymbol{k}/|\boldsymbol{k}|^2 + \varrho\hat{\boldsymbol{z}} \times \boldsymbol{k}, \tag{B 2}$$

where $\boldsymbol{\Gamma}$ is the (absolute) vorticity of the equilibrium flow. Owing to the contribution of buoyancy in that equation, we note in passing that irrotational trajectories may be unstable with density stratification. Now, (B 1*b*) with $B=0$ and (B 2) projected on the vertical axis yield respectively

$$\dot{\varrho} = N^2 v_z, \quad \dot{\omega}_z = \Gamma k_z v_z, \tag{B 3}$$

where the subscript z denotes the vertical component. As a consequence, $\Gamma k_z \varrho - N^2\omega_z$ is a Lagrangian invariant, i.e. an integral of the motion. Note that this property may also be proved by conservation of potential vorticity. If a trajectory is unstable, this integral must be zero, so that

$$\Gamma k_z \varrho = N^2 \omega_z. \tag{B 4}$$

Indeed, both Γ and k_z are constant along the trajectories of the equilibrium flow; therefore, if ϱ and ω_z grow exponentially as $t \to +\infty$, they must vanish when $t \to -\infty$ and the conclusion follows.

Now, it may be shown from (B 1*a*) and the incompressibility condition $\boldsymbol{k} \cdot \boldsymbol{v} = 0$ that the vertical component of the velocity disturbance is governed by

$$\dot{v}_z = -2k_z^2 \frac{\boldsymbol{k}_h^T \boldsymbol{L} \boldsymbol{k}_h}{|\boldsymbol{k}_h|^2|\boldsymbol{k}|^2} v_z - 2k_z \frac{\boldsymbol{k}_h^T \boldsymbol{H} \boldsymbol{k}_h}{|\boldsymbol{k}_h|^2|\boldsymbol{k}|^2}\omega_z - \frac{|\boldsymbol{k}_h|^2}{|\boldsymbol{k}|^2}\varrho, \quad \boldsymbol{H} = \boldsymbol{L}\begin{pmatrix} 0 & 1 \\ -1 & 0 \end{pmatrix}. \tag{B 5}$$

Thus, the local stability problem is now reduced to a system of three differential equations (B 3) and (B 5) for the variables (ϱ, ω_z, v_z).

One of these variables may be eliminated thanks to (B 4) and the problem is reduced to two equations. Following Bayly *et al.* (1996), it is convenient to introduce

$$p = -k_z v_z |\boldsymbol{k}|/|\boldsymbol{k}_h| \quad \text{and} \quad q = \omega_z |\boldsymbol{k}|/|\boldsymbol{k}_h|.$$

After some algebra, the resulting system of equations may be written as

$$\begin{pmatrix} \dot{p} \\ \dot{q} \end{pmatrix} = \begin{pmatrix} \dot{K} & D \\ -\Gamma & -\dot{K} \end{pmatrix} \begin{pmatrix} p \\ q \end{pmatrix},$$

where Γ is the basic vorticity and

$$K = \ln \frac{|\boldsymbol{k}_h|}{|\boldsymbol{k}|}, \quad D = 2k_z^2 \frac{\boldsymbol{k}_h^T \boldsymbol{H} \boldsymbol{k}_h}{|\boldsymbol{k}_h|^2|\boldsymbol{k}|^2} + \frac{N^2}{\Gamma}\frac{|\boldsymbol{k}_h|^2}{|\boldsymbol{k}|^2}.$$

Therefore, since $\dot{\Gamma} = 0$, this system may be written as $\ddot{q} + (\ddot{K} - \dot{K}^2 + \Gamma D)q = 0$ which after some further calculations yields (7.1).

Appendix C. Steady vortices in strain fields

We prove that the vortex patches described by (8.1) are steady and may be matched with a potential steady flow which behaves as a multipolar strain field at infinity. From (8.1) with $|\xi| \leqslant 1$, the position $Z(t, \xi, \bar{\xi})$ and complex velocity $W(t; \xi, \bar{\xi}) = \partial_t \bar{Z}$ of a fluid particle inside the vortex may be represented as

$$Z(\beta, \bar{\beta}) = \beta + S\bar{\beta}^{n-1}/(n-1), \quad W(\beta, \bar{\beta}) = -\mathrm{i}\omega(\bar{\beta} - S\beta^{n-1})/n, \tag{C 1a, b}$$

where $\beta = \xi e^{i\omega t/n}$. If we choose the complex parameter β in the interior of the unit disk, $|\beta| \leqslant 1$, and the complex coordinate $z = x + iy$ related to β by

$$z = \beta + S\bar{\beta}^{n-1}/(n-1), \tag{C 2}$$

then (C 1b) and (C 2) provide an implicit representation of the complex Eulerian velocity field: $W(z, \bar{z}) = U - iV$. Time being eliminated from the Eulerian representation of the velocity field, the corresponding flows are therefore steady.

In the exterior region, the Eulerian complex velocity field is represented as

$$W_{ext}(\eta) = -i\omega(\eta^{-1} - S\eta^{n-1})/n \quad \text{where} \quad z = \eta + S\eta^{1-n}/(n-1) \quad \text{and} \quad |\eta| > 1. \tag{C 3}$$

Since W_{ext} depends implicitly on z, and not on $\bar{z}$ nor t, the flow in the exterior region is stationary and irrotational. Continuity of the velocity field across the vortex boundary is easily checked from (C 1) and (C 3), since β and η may be written as $e^{i\chi}$ ($\chi \in [0, 2\pi]$) on the unit circle.

Far from the vortex ($|z| \to \infty$), $z \sim \eta$ and $W_{ext} \sim -i\omega/(nz) + i\omega S z^{n-1}/n$: this is the superposition of a point vortex with circulation $2\pi\omega/n$ and of an irrotational strain field. Thus the exact solution (8.1) generalizes the Moore–Saffman steady elliptical equilibrium in a strain field.

It is finally of interest to show that when $S \ll 1$, these flows are connected to the uniform multipolar vortices described by Eloy & Le Dizès (2001). Indeed, relation (C 2) between the complex coordinate z and the auxiliary parameter β may be easily reversed for small S. It gives, to a first approximation, $\beta = z - S\bar{z}^{n-1}/(n-1)$, so that the complex velocity (C 1b) is

$$W(z, \bar{z}) = -i\omega(\bar{z}/n - Sz^{n-1}/(n-1)). \tag{C 4}$$

The flow being incompressible, it may be characterized by a stream function defined by the usual relations $U = \partial_y \Psi$ and $V = -\partial_x \Psi$. In terms of the complex coordinates, it is not difficult to show that these relations are $\partial_z \Psi = -\frac{1}{2} i W$ and $\partial_{\bar{z}} \Psi = \frac{1}{2} i \bar{W}$. Upon integration, the stream function related to (C 4) therefore becomes

$$\Psi(z, \bar{z}) = -\frac{\omega}{2n}\left(|z|^2 - S\frac{z^n + \bar{z}^n}{n-1}\right) = -\frac{\omega}{n}\left(\frac{r^2}{2} - \frac{Sr^n}{n-1}\cos n\theta\right) = \Psi(r, \theta), \tag{C 5}$$

with $z = re^{i\theta}$. This is the solution discussed in Le Dizès (2000).

Recall that (C 5) is also an exact solution of Euler equations. However, contrary to (C 1), its vorticity is uniform ($\Gamma = 2\omega/n$) and it is not known if (C 5) may be matched with an external potential strain field for any S. When $S \ll 1$, such a construction is possible, as mentioned by Eloy & Le Dizès. Their results may be recovered directly from our potential solution (C 3). Indeed, at first order in S we get $\eta = z - Sz^{1-n}/(n-1)$. Therefore, the external stream function may be evaluated and is, when $S \ll 1$, in agreement with Eloy & Le Dizès

$$\Psi_{ext}(r, \theta) = -\frac{\omega}{n}\left(\ln r - \frac{S}{n}\left(r^n + \frac{r^{-n}}{n-1}\right)\cos n\theta\right).$$

Note finally that in the case of freely rotating vortex patches in a potential flow at rest at infinity, the solution of Abrashkin & Yakubovich (2.3) with (3.1) may be characterized, when $S \ll 1$, by the following stream function:

$$\Psi(r, \theta, t) = -\frac{\omega}{n}\left(\frac{nr^2}{2} - \frac{Sr^n}{n-1}\cos n(\theta - \Omega_n t)\right) \quad \text{with} \quad \Omega_n = \omega(1 - 1/n).$$

It corresponds to a Rankine vortex with vorticity 2ω disturbed by planar Kelvin modes with n-fold symmetry that rotates with angular velocity Ω_n (Saffman 1992, § 9.4).

REFERENCES

ABRASHKIN, A. A. & YAKUBOVICH, E. I. 1984 Planar rotational flows of an ideal fluid. *Sov. Phys. Dokl.* **29**, 370–371.

BASSOM, A. P. & GILBERT, A. D. 1998 The spiral wind-up of vorticity in an inviscid planar vortex. *J. Fluid Mech.* **371**, 109–140.

BAYLY, B. J. 1987 Three-dimensional instabilities in quasi-two-dimensional inviscid flows. In *Nonlinear Wave Interactions in Fluids* (ed. R. W. Miksad *et al.*), pp. 71–77. ASME.

BAYLY, B. J., HOLM, D. D. & LIFSCHITZ, A. 1996 Three-dimensional stability of elliptical vortex columns in external strain flows. *Phil. Trans. R. Soc. Lond.* A **354**, 895–926.

BAYLY, B. J., ORSZAG, S. A. & HERBERT, T. 1988 Instability mechanisms in shear-flow transition. *Annu. Rev. Fluid Mech.* **20**, 359–391.

BENDER, C. M. & ORSZAG, S. A. 1978 *Advanced Mathematical Methods for Scientists and Engineers.* McGraw-Hill.

CAMBON, C., BENOIT, J.-P., SHAO, L. & JACQUIN, L. 1994 Stability analysis and large eddy simulation of rotating turbulence with organized eddies. *J. Fluid Mech.* **278**, 175–200.

CAMBON, C. & SCOTT, J. F. 1999 Linear and nonlinear models of anisotropic turbulence. *Annu. Rev. Fluid Mech.* **31**, 1–53.

CRAIK, A. D. D. 1989 The stability of unbounded two- and three-dimensional flows subject to body forces: some exact solutions. *J. Fluid Mech.* **198**, 275–292.

DRITSCHEL, D. G. 1998 On the persistence of non-axisymmetric vortices in inviscid two-dimensional flows. *J. Fluid Mech.* **371**, 141–155.

ECKHOFF, K. S. & STORESLETTEN, L. 1978 A note on the stability of steady inviscid helical gas flows. *J. Fluid Mech.* **89**, 401–411.

ELOY, C. & LE DIZÈS, S. 2001 Stability of the Rankine vortex in a multipolar strain field. *Phys. Fluids* **13**, 660–676.

FRIEDLANDER, S. 2001 On nonlinear instability and stability for stratified shear flow. *J. Math. Fluid Mech.* **3**, 82–97.

FRIEDLANDER, S. & LIPTON-LIFSCHITZ, A. 2003 Localized instabilities in fluids. In *Handbook of Mathematical Fluid Dynamics*, vol. 2 (ed. S. Friedlander & D. Serre), pp. 289–354. North-Holland.

FRIEDLANDER, S. & VISHIK, M. M. 1991 Instability criteria for the flow of an inviscid incompressible fluid. *Phys. Rev. Lett.* **66**, 2204–2206.

HUERRE, P. & ROSSI, M. 1998 Hydrodynamic instabilities in open flows. In *Hydrodynamics and Nonlinear Instabilities* (ed. C. Godrèche & P. Manneville), pp. 81–294. Cambridge University Press.

KERSWELL, R. R. 2002 Elliptical instability. *Annu. Rev. Fluid Mech.* **34**, 83–113.

LEBLANC, S. 2003 Internal wave resonances in strain flows. *J. Fluid Mech.* **477**, 259–283.

LEBLANC, S. 2004 Local stability of Gerstner's waves. *J. Fluid Mech.* **506**, 245–254.

LEBLOND, P. H. & MYSAK, L. A. 1978 *Waves in the Ocean.* Elsevier.

LE DIZÈS, S. 2000 Three-dimensional instability of a multipolar vortex in a rotating flow. *Phys. Fluids* **12**, 2762–2774.

LIFSCHITZ, A. 1994 On the instability of certain motions of an ideal incompressible fluid. *Adv. Appl. Maths* **15**, 404–436.

LIFSCHITZ, A. & HAMEIRI, E. 1991 Local stability conditions in fluid dynamics. *Phys. Fluids* A **3**, 2644–2651.

MIYAZAKI, T. 1993 Elliptical instability in a stably stratified rotating fluid. *Phys. Fluids* A **5**, 2702–2709.

MIYAZAKI, T. & FUKUMOTO, Y. 1992 Three-dimensional instability of strained vortices in a stably stratified fluid. *Phys. Fluids* A **4**, 2515–2522.

MIYAZAKI, T., IMAI, T. & FUKUMOTO, Y. 1994 Three-dimensional instability of Kirchhoff's elliptic vortex. *Phys. Fluids* **7**, 195–202.

Robinson, A. C. & Saffman, P. G. 1984 Three-dimensional stability of an elliptical vortex in a straining field. *J. Fluid Mech.* **142**, 451–466.

Saffman, P. G. 1992 *Vorticity Dynamics*. Cambridge University Press.

Vladimirov, V. A. & Il'in, K. I. 1988 Three-dimensional instability of an elliptic Kirchhoff vortex. *Fluid Dyn.* **23**, 356–360.

Waleffe, F. 1990 On the three-dimensional instability of strained vortices. *Phys. Fluids* A **2**, 76–80.

Yakubovich, E. I. & Zenkovich, D. A. 2001 Matrix approach to Lagrangian fluid dynamics. *J. Fluid Mech.* **443**, 167–196.

Zeitlin, V. 1991 On the backreaction of acoustic radiation for distributed two-dimensional vortex structures. *Phys. Fluids* A **3**, 1677–1680.